RESEARCH ACTIVITIES III
Department of Electronic Structure

III-A States of Molecular Associates in Solutions

States of molecular association particularly in aqueous solutions are of great importance in understanding the role of molecules in living organism. Our recent studies of low frequency Raman spectroscopy of binary aqueous solutions of alcohols and carboxylic acids have shown that these amphiphilic molecules form microphases of clusters with the same solute species. This observation is in accord with the results of the ultrasonic absorption measurement of the binary mixtures. Kaatze and his coworkers found that acetic acid/water mixtures shows two relaxation terms attributed to the existence of two microphases, one with high and the other with low water contents. The water rich phase was assumed to fill the space between the acid-rich microphase aggregates. They also reported that the fluctuation correlation lengths in monohydric alcohol/water mixtures were expected to exceed some molecular diameters in contrast to much longer lengths expected for acid-rich phases in carboxylic acid/water mixtures. Low frequency Raman spectroscopy provides information on local structure of solutions coupled with hindered translational and librational motions. The Raman signals originating from dipole-induced dipole interaction are dominated with the interaction between the neighboring molecules. Theoretical prediction of intermolecular vibrational frequencies and Raman intensities is also applied for the assignment of observed Raman bands. These results are discussed not only with the mass spectrometric measurement of the clusters isolated from the liquid droplets through adiabatic expansion in vacuum, but also with the X-ray diffraction studies.

III-A-1 Raman Spectroscopic Study on Acetic Acid Clusters in Aqueous Solutions: Dominance of Acetic-Acid Association Producing Micro-Phases

NISHI, Nobuyuki; NAKABAYASHI, Takakazu; KOSUGI, Kentaroh[1]
([1]GUAS)

[*J. Phys. Chem. A* in press]

With the addition of water into liquid acetic acid, the C=O stretching vibration band of acetic acid shows high frequency shift from 1665 cm^{-1} to 1715 cm^{-1}. This means that the hydrogen-bond of the C=O group of acetic acid is not so strong as those seen in liquid acetic acid or in CCl_4 solution (in which the band appears at 1668 cm^{-1}). A bent type hydrogen-bond is accountable for this observation. On the other hand, the increase of acetic acid in water drastically decreases the intensity of the hydrogen-bonded O-H stretching Raman band of water at 3200 cm^{-1}. This suggests that acetic acid breaks the hydrogen-bond networks of water. Low frequency $R(\overline{\nu})$ spectra of acetic acid/water binary solutions are reexamined with new experimental data and ab initio molecular orbital analysis of intermolecular vibrational modes. The $R(\overline{\nu})$ spectrum of the aqueous mixture at $x_A = 0.5$ bears a very close resemblance to that of the acetic acid/methanol mixture with $x_A = 0.5$, indicating that the molecular complexes responsible to the Raman spectra are acetic acid clusters. The calculated low-frequency Raman feature of a side-on type dimer with bent-type hydrogen-bonds based on ab initio molecular orbital theory reproduces the observed Raman pattern nicely. Any evidence of the formation of stable acid-water pairs is not found in the low frequency Raman spectra. Furthermore, an isosbestic point is seen in the region of $0.1 \leq x_A$ (mole fraction of acetic acid) ≤ 0.5, and another one is also observed in $0.5 \leq x_A \leq 1.0$. The observed spectra in the region of $0 < x_A < 0.5$ are reproduced simply by linear combinations of the pure water spectrum and the spectrum at $x_A = 0.5$. Figure 1 shows some examples of the spectral analyses. These results strongly suggest the presence of the two microphases with homogeneously associated molecules: a water cluster phase and an acetic acid cluster phase. The spectral change in $0.5 < x_A < 1.0$ is attributed to the coexistence of the acetic acid cluster phase in aqueous environment and the acid associated phase characteristic of liquid acetic acid.

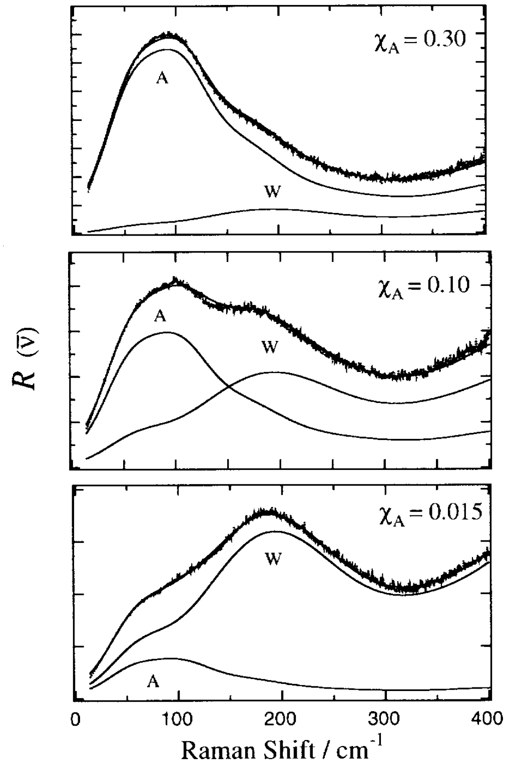

Figure 1. Decomposition of the observed $R(\overline{\nu})$ spectra of the binary solutions with x_A = 0.015, 0.10 and 0.30 into linear combination of the $R(\overline{\nu})$ spectra of pure water and the mixture with x_A = 0.5. The sum spectra calculated by a least square fitting are shown with solid lines.

III-A-2 Structures and Energies of Acetic Acid Aggregates in Aqueous Solution Studied by the RISM-SCF Method

NAKABAYASHI, Takakazu; SATO, Hirofumi; NISHI, Nobuyuki; HIRATA, Fumio

Acetic acid has been thought to form a cyclic dimer having a planar ring structure of C_{2h} symmetry in aqueous solution. From an analysis of Raman spectra of acetic acid/water binary solutions, however, we have suggested that a side-on dimer, not the cyclic dimer, is most likely for acetic acid in aqueous solution (structures of both the dimers are depicted in Figure 1). This means that the side-on dimer is more stable than the cyclic dimer in aqueous solution, although the cyclic structure is quite stable in the gas phase. In the present study, we calculate the hydrogen-bonding energies and structures of the cyclic dimer and the side-on dimer in aqueous solution by the RISM-SCF method. The advantage of the RISM-SCF method is to maintain the molecular aspects of solvents and thus to appropriately describe local interactions such as hydrogen bonds. The total energies and their energy components calculated for the monomer and the dimer species are collected in Table 1. The total energy (E_{tot}) in the RISM-SCF theory is defined as the sum of the following three energy components: (1) the electronic energy of solute molecule in the gas phase (E_{iso}), (2) the reorganization energy arising from the relaxation of the electronic structure and the molecular geometry upon transferring solute from gas to aqueous solution (E_{reorg}), and (3) the excess chemical potential coming from solute-solvent interaction ($\Delta\mu$). The RISM-SCF calculations predict that the excess chemical potential of the side-on dimer is lower by 7.0 kcal/mol than that of the cyclic dimer. From the decomposition of the excess chemical potential into its constituents, the contribution from one of the carbonyl-oxygen atoms, which is free from the hydrogen bonding interaction with the other acetic acid molecule, is found to be much greater than the other atoms. Owing to such a stabilization in the side-on dimer, the energy difference between the two clusters is calculated to be reduced in solution; 2.0 kcal/mol in solution compared with 8.1 kcal/mol in the gas phase. Since the dipole moment of the side-on dimer is estimated to be 4.0 Debye in contrast to the null dipole moment of the cyclic dimer, the dipole-dipole interaction between the side-on dimers is expected to be sufficiently large. It is thus conceivable that the interaction energy between the side-on dimers exceeds over that between the cyclic dimers and contributes the stability of the side-on dimers in aqueous solution.

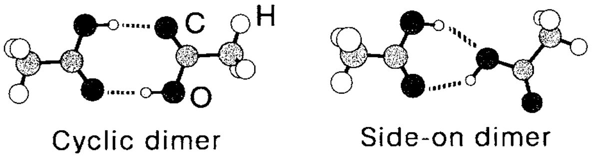

Figure 1. Structures of acetic acid dimers.

Table 1. Total energies and their energy components of acetic acid monomer and dimers in aqueous solution at the HF/DZP level.

	E_{total} (hartress)	E_{gas} (hartless)	E_{reorg} (kcal/mol)	$\Delta\mu$ (kcal/mol)
cis-Monomer	-227.8648503	-227.8721748	3.94	0.66
Cyclic dimer	-455.7318117	-455.7672506	4.05	18.19
Side-on dimer	-455.7270251	-455.7543088	5.96	11.16

III-A-3 Rayleigh Wing Spectra and Microphase Formation

NISHI, Nobuyuki; NAKABAYASHI, Takakazu; KOSUGI, Kentaroh[1]
([1]GUAS)

Motion of molecular clusters causing dipole-dipole or dipole-induced dipole interaction between the clusters can be observed in a very low frequency Raman spectrum of a solution. Rousset *et al.*1) assumed that the low frequency temperature-dependent Raman scattering comes from oscillations of transient water aggregates with a somewhat ordered structure on the basis of the Raman studies of nuclei in glasses and silica particles in aerogels. Orientational relaxation coupled with long range dipole-dipole interaction can be also responsible to the Raman spectrum at the low frequency of 1–20 cm^{-1}. Figure 1 shows Bose-Einstein (BE) corrected very low frequency Raman spectra of water (spectrum A), aqueous mixtures with x_{A} = 0.0075 (spectrum B) and 0.07 (spectrum C). As reported by Rousset *et al.*,1) the water spectrum at 298 K exhibits a hump at 10 cm^{-1}. This signal is temperature dependent in intensity and the position. The frequency increases with increasing temperature and falls to zero at –30 °C. Addition of a small amount of acetic acid in water enhances the wing intensity drastically, particularly in the region from 4 to 8 cm^{-1}. The 10 cm^{-1} component in the water spectrum in the figure must be related to this orientational relaxation of large water clusters. Rousset *et al.* estimated the average size of the clusters at room temperature to be 11 Å. In the aqueous mixture of acetic acid, orientational relaxation of the clusters is expected to take much longer time than that of water because of their longer sizes and larger dipole moments of the side-on type acetic acid dimer and higher clusters with this dimer unit. The clusterization of acetic acid molecules with large dipole-dipole interaction thus provides us a reasonable elucidation for the enhanced activity of the very low frequency Raman component as compared with that of water. The microphase model is in accord with the present observation of the enhancement in the very low frequency component of the Raman spectra of the mixtures. As expected from the crystal structure of acetic acid, dipole-dipole interaction could be dominated in the acetic acid clusters elongating the lifetimes of the clusters in aqueous solutions.

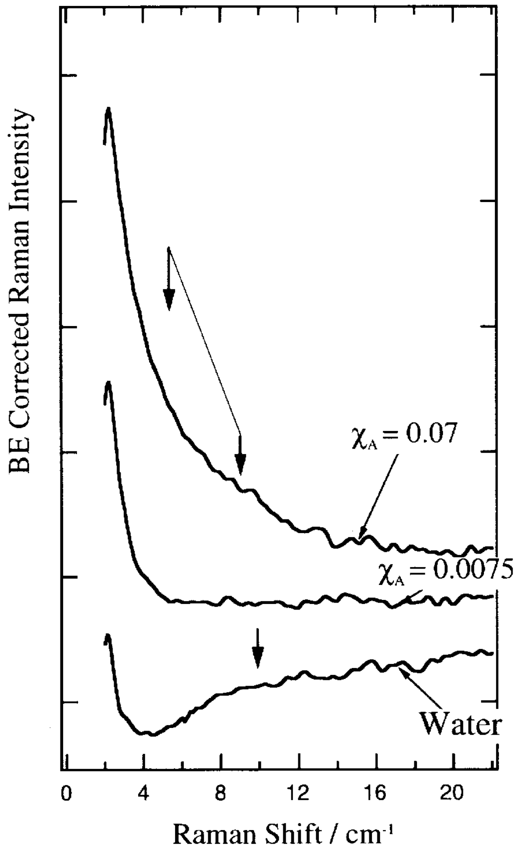

Figure 1. Mixing ratio dependence of the $R(\bar{\nu})$ spectra in acetic acid-water binary system.

III-A-4 Structures of Clusters in Methanol-Water Binary Solutions Studied by Mass Spectrometry and X-ray Diffraction

TAKAMUKU, Toshiyuki[1]; YAMAGUCHI, Toshio[2]; ASATO, Masaki[3]; MATSUMOTO, Masaki[3]; NISHI, Nobuyuki
([1]Saga Univ.; [2]Fukuoka Univ.; [3]Kyushu Univ.)

[*J. Phys. Chem. B* submitted]

The structure of clusters in methanol-water binary solutions has been investigated as a function of methanol mole fraction, x_M, by mass spectrometry on clusters isolated from submicron droplets by adiabatic expansion in vacuum and by X-ray diffraction on the bulk binary solutions. The mass spectra have shown that the average hydration number, $<n_m>$, for m-mer methanol clusters, M_mW_n (M = methanol, and W = water), decreases with increasing mole fraction of methanol, accompanied with two inflection points approximately at $x_M = 0.3$ and 0.7. Figure 1 shows the plots of average hydration numbers, $<n_m>$, for methanol m-mer hydrates with m = 6, 8, 10 and 12. The X-ray diffraction data have also revealed a similar change in the number of hydrogen bonds per water and/or methanol oxygen atom at 2.8 Å to that found from mass spectrometry. On the basis of the results from the two methods, the most likely models of clusters formed in the binary solutions have been proposed; at $0 \le x_M \le 0.3$ the tetrahedral-like water clusters are the main species, at $0.3 \le x_M \le 0.7$ chain clusters of methanol molecules are gradually evolved with increasing methanol content, and at $x_M \ge 0.7$ chain clusters of methanol molecules become predominant. A comparison of the present results on the methanol-water mixtures with those of ethanol-water ones has shown that the tetrahedral-like water structure is broken down at a lower mole fraction of 0.2 and more sharply in the ethanol-water mixtures than in the methanol-water ones due to the large hydrophobic effect of ethanol. The behavior of the heat of mixing with varying alcohol concentration in the methanol-water mixtures is consistent with that of the average clusters formed in the mixtures, and thus anomalies in the physico-chemical data of alcohol-water probably originate from clusters formed in the mixtures.

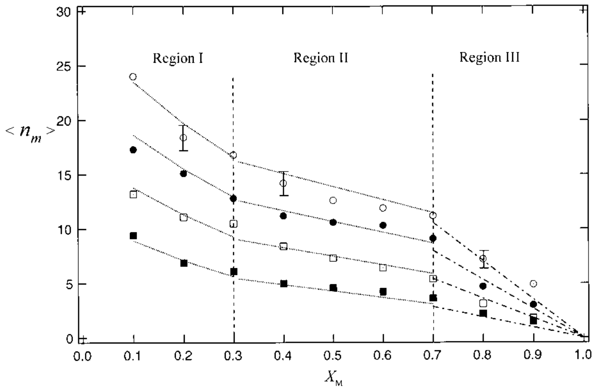

Figure 1. Plots of average hydration numbers, $<n_m>$, for methanol m-mer hydrates with m = 6 (■), 8 (□), 10 (●) and 12 (○) as functions of methanol mole fractions (x_m). Dotted lines were obtained from the equations: $<n_m> = 3(m - 0.5)(x_M - 0.3)^2 + 0.45(m - 3.8)$ for $0 \le x_M \le 0.3$, $<n_m> = m\,(x_M - 0.3)^2 + 1.4(m - 3.8)$ for $0.3 \le x_M \le 0.7$, and $<n_m> = 4.3(m - 3.8)x_M$ for $x_M \ge 0.7$.

III-A-5 Structure and Dynamics of 1,4-Dioxane-Water Binary Solutions Studied by X-ray diffraction, Mass Spectrometry, and NMR Relaxation

TAKAMUKU, Toshiyuki[1]; YAMAGUCHI, Atsushi[1]; TABATA, Masaaki[1]; NISHI, Nobuyuki; YOSHIDA, Koji[2]; WAKITA, Hisanobu[2]; YAMAGUCHI, Toshio[2]
([1]Saga Univ.; [2]Fukuoka Univ.)

[*J. Mol. Liq.* in press]

The structure of clusters formed in 1,4-dioxane-water binary solutions has been investigated at ambient temperature as a function of 1,4-dioxane concentration by X-ray diffraction for the corresponding solutions and by mass spectrometry for liquid droplets formed in vacuum from the liquid mixtures by an adiabatic expansion method. The ^{2}H spin-lattice relaxation times of D_2O and 1,4-dioxane-d_8 molecules in 1,4-dioxane-water binary solutions have also been measured at 30 °C over a whole range of 1,4-dioxane mole fraction. It has been found from the analysis of X-ray radial distribution functions that the number of hydrogen-bonds per water and 1,4-dioxane oxygen atom decreases with increasing 1,4-dioxane mole fraction X_{dio}, accompanied by two inflection points at approximately $X_{\mathrm{dio}} = 0.1$ and 0.3: at $X_{\mathrm{dio}} \geq 0.3$ the inherent structure of 1,4-dioxane is mostly observed, water molecules probably involved in the structure by hydrogen bonding, and at $0.15 \leq X_{\mathrm{dio}} \leq 0.2$ both structures of water and 1,4-dioxane are ruptured to form small binary clusters of one or two dioxane and several water molecules. The mass spectra have revealed that at $X_{\mathrm{dio}} = 0.01$ water clusters W_n (W = water) are mostly formed, but with increasing X_{dio} to 0.4 the water cluster reduced with evolving 1,4-dioxane clusters $\mathrm{D_mW_n}$ (D = 1,4-dioxane). The ^{2}H spin-lattice relaxation data of D_2O molecules in the mixtures showed that the rotation of water molecules is gradually retarded with increasing X_{dio} to 0.3, where the rotation is the slowest, and is then gradually accelerated with further increase in X_{dio}. The corresponding data of 1,4-dioxane-d_8 molecules showed a similar tendency, but the slowest motion observed at $X_{\mathrm{dio}} = 0.2$. The present microscopic cluster structure and dynamic properties of the mixtures are discussed in connection with the heat of mixing, viscosity, and hydrophobic hydration.

III-B Ultrafast Dynamics of Photoexcited Molecules Studied by Transient Absorption and Transient Raman Spectroscopy Methods

Ultrafast transient absorption spectroscopy and transient Raman spectroscopy is now an universal and popular method for the study of reaction pathways induced by electronic or vibrational excitation of organic or metal complex molecules. We have constructed a new femto-pico synchronized multi-laser beam system. This unique system is open for collaborations in the field of molecular science.

III-B-1 Construction of a Tunable and Synchronized Picosecond-Femtosecond Double Laser System for the Study of Photodissociation Dynamics of Molecular Clusters in Solution

NAKABAYASHI, Takakazu; SATO, Shin-ichiro; INOKUCHI, Yoshiya; WATANABE, Kazuo; SAKAI, Makoto; FUJII, Masaaki; NISHI, Nobuyuki

Many time-resolved spectroscopic techniques require two broadly and independently tunable, synchronized light pulses with sufficient pulse energies. Since femtosecond time resolution simultaneously implies the loss of frequency resolution, a complementary use of picosecond and femtosecond pulse lasers is attractive for studying molecular dynamics. In order to meet these requirements, we have first constructed a tunable and synchronized picosecond-femtosecond double laser system, which is schematically shown in Figure 1. Two independently tunable OPAs are pumped by the output from a picosecond regenerative amplifier operating at 1 kHz repetition rate, 3 mJ pulse energy with 4 ps pulse duration and at 790 nm. By using sum- and difference frequency mixings, we have obtained the continuous tuning of light between 189 and 11200 nm with keeping microjoule pulse energy. Another OPA is excited by the output from a femtosecond regenerative amplifier (1 kHz, 2 mJ, 200 fs, 800 nm) to generate femtosecond pulses over a 300-10000 nm spectral range. A portion of the output from the femtosecond regenerative amplifier is separated and used for harmonic generations. The pulse energy obtained is about 120 µJ for the third harmonic and about 10 µJ for the fourth harmonic, when amplified pulses with 1 mJ pulse energy are used. Two femtosecond mode-locked Ti:sapphire lasers are used to seed the picosecond and femtosecond regenerative amplifiers, respectively. The phase-detection method is adopted to lock the timing of the femtosecond lasers. A typical cross correlation function of pulses from the femtosecond lasers is shown in Figure 2a. The FWHM of the cross-correlation is observed to be 2.5 ps, which corresponds to the timing jitter between pulses from the femtosecond lasers. The two regenerative amplifiers are excited by the output from Q-switched cw Nd:YLF lasers, which are triggered externally by the output from one of the femtosecond laser. Figure 2b shows the cross correlation function of pulses from the regenerative amplifiers. The FWHM of the cross-correlation is found to be about 8 ps, indicating that the regenerative amplifiers are synchronized with the timing jitter of several picoseconds. The femtosecond regenerative amplifier has also been modified to be further excited by a Q-switched pulsed Nd:YAG laser to generate amplified pulses with 10 mJ pulse energy at 10 Hz repetition rate. We have observed time-resolved absorption and Raman spectra of some polyatomic molecules by using this laser system.

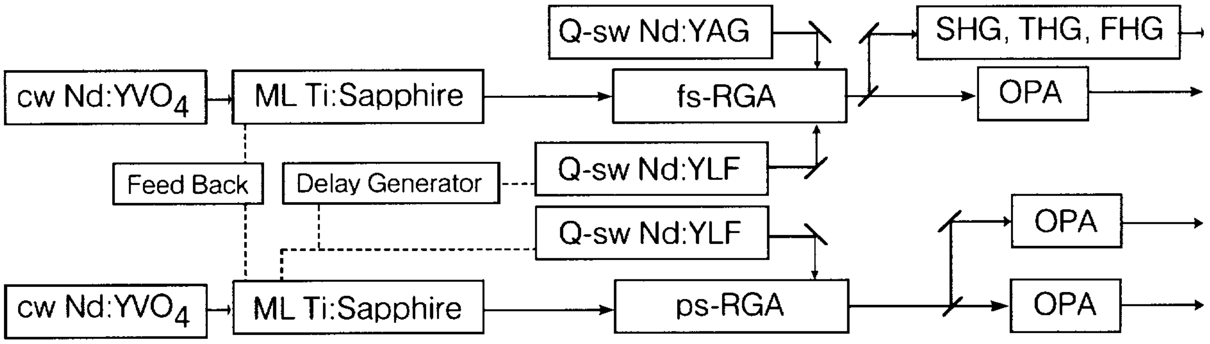

Figure 1. Block diagram of the picosecond-femtosecond double laser system.

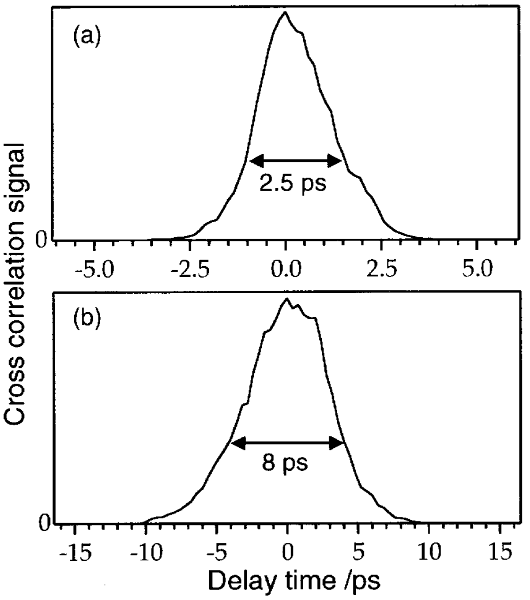

Figure 2. Cross correlation functions observed for pulses from (a) the femtosecond mode-locked lasers and (b) the picosecond and femtosecond regenerative amplifiers.

III-C Spectroscopic and Dynamical Studies on Charge Delocalization and Charge Transfer in Aromatic Molecular Cluster Ions

Charge transfer processes resulting in dynamical charge delocalization such as consecutive proton or electron hopping in molecular clusters and even in pure liquids are highly interesting in relation to the charge transportation in insulating materials. Not only in aromatic molecular liquids but also in pure water itself electric conductivity is very low when they do not contain impurities of ionic atoms or molecules. It is possible to control charge hopping with near infrared photons in such aromatic liquids. Here we investigate the role of impurity or neighboring molecules in changing the electronic properties of benzene cluster cations.

III-C-1 Photodissociation Spectroscopy of Benzene-Acetic acid Mixed Cluster Ions

KOSUGI, Kentaroh; INOKUCHI, Yoshiya; NISHI, Nobuyuki

It is now well known that the charge resonance interactions between the π-electron systems dominate the structures of the benzene cluster ions. On the other hand, the π electrons of the carboxyl group of acetic acid is expected to show strong interaction with the π-electron systems of the aromatic cations. In this study, we measure the photodissociation spectra of benzene-acetic acid mixed cluster ions for investigating the positive charge localization and the structure of the binary complexes.

The experiment is done by using a tandem mass spectrometer coupled with infrared (IR), near IR, and visible lasers. Figure 1(a) displays the photodissociation spectra of $[(C_6H_6)_2(CH_3COOH)_n]^+$ with n = 1–4 in the near IR region. All the spectra show very broad bands with a maximum at 920 nm. Since the spectral features well resemble that of benzene dimer cation, we ascribe the bands to the charge resonance bands of benzene dimer ion cores in $[(C_6H_6)_2(CH_3COOH)_n]^+$. In the mixed cluster ions, the positive charge is localized in the benzene dimer site. The photodissociation spectrum in the IR region is thought to be a much better probe of the cluster structure. Figure 1(b) shows the photodissociation spectrum of $[(C_6H_6)_2(CH_3COOH)_1]^+$ in the

IR region. Three bands emerge at 3084, 3585, and 3627 cm^{-1}. According to the spectrum of $[(C_6H_6)_2(CD_3COOD)_1]^+$, the band at 3084 cm^{-1} is assigned to the CH stretching vibration of the benzene dimer ion core, and the bands at 3585 and 3627 cm^{-1} are to the OH stretching vibrations of acetic acid. The two OH stretching vibrations imply the existence of two isomers. Possible isomers are *cis*- and *trans*-acetic acid molecules in $[(C_6H_6)_2(CH_3COOH)_1]^+$. In the gas phase, the free OH stretching vibration of a *cis*-acetic acid monomer emerges at 3583 cm^{-1}. Theoretical investigation of the acetic acid monomer by Turi et al. implied that the OH stretching vibration of *trans*-acetic acid has higher frequency than that of the *cis*-acetic acid. According to the facts, we can assign the band at 3585 cm^{-1} to the OH stretching vibration of $[(C_6H_6)_2(cis\text{-}CH_3COOH)_1]^+$, and the band at 3627 cm^{-1} to that of $[(C_6H_6)_2(trans\text{-}CH_3COOH)_1]^+$. In these ions, the acetic acid points the lone pair electrons on the oxygen of the carbonyl group to the benzene dimer ion core, and the OH group of the acetic acid is free from any binding. The benzene dimer ion core makes the *trans*-acetic acid comparatively stable with the *cis*-acetic acid, and the OH vibrations of both *cis*- and *trans*-acetic acid molecules in $[(C_6H_6)_2(CH_3COOH)_1]^+$ are observed in the IR spectrum.

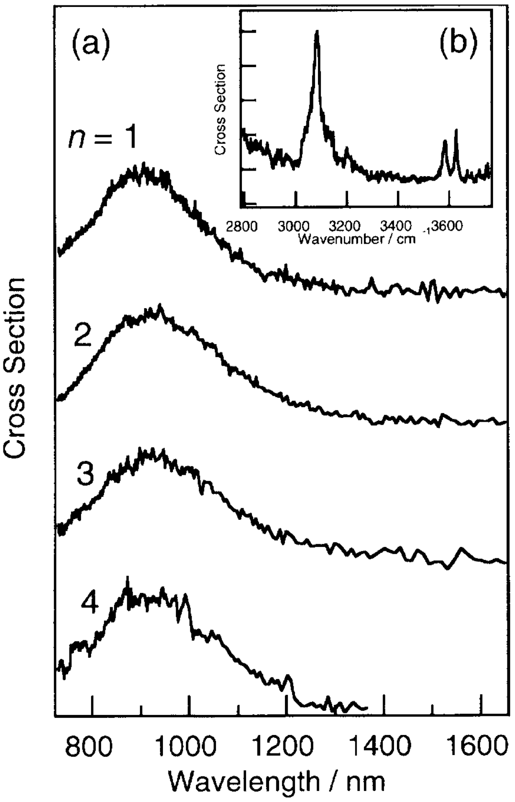

Figure 1. (a) Photodissociation spectra of $[(C_6H_6)_2(CH_3COOH)_n]^+$ with n = 1–4 in the near IR region. (b) Photodissociation spectrum of $[(C_6H_6)_2(CH_3COOH)_1]^+$ in the IR region.

III-C-2 Structural Isomers of Benzene-Phenol Mixed Dimer Cation

INOKUCHI, Yoshiya; NISHI, Nobuyuki

The benzene dimer cation with a parallel sandwich structure has a broad and strong absorption band at 920 nm. This band is assigned to the charge resonance (CR) band. The existence of the CR band implies that the positive charge is delocalized in the parallel dimer. On the other hand, the benzene-phenol mixed dimer cation does not show any strong band in the near infrared (IR) region. Therefore, the structure of the mixed dimer cation is thought to be dominated with the hydrogen bonding of the OH group to the π electrons of the benzene. We measure the photodissociation spectra of ordinary and deuterated benzene-phenol mixed dimer cations in the IR region in order to get information on their structures with the help of theoretical calculation.

Figure 1 displays the photodissociation spectra of the benzene-phenol mixed dimer cations. The spectrum at the top is similar to that measured by Mikami *et al.* There are two maxima at 3200 and 3060 cm^{-1}. These bands could be assigned to the OH stretching vibration and CH stretching vibrations of the mixed dimer cation. We also measure the spectrum of the deuterated mixed dimer cation, $[(C_6D_6)(C_6D_5OH)]^+$, showed in the bottom of Figure 1. The spectral feature of the deuterated cation is almost the same as that of the non-deuterated one. Thus, we can confirm that both bands are ascribed to the OH stretching vibrations. Appearance of the two OH stretching vibrations suggests that there are two structural isomers. The frequency of 3060 cm^{-1} is very low as a normal OH stretching frequency, even for a hydrogen-bonded dimer. One possibility is a proton transferred ion complex, $[(C_6H_6\text{-}H^+)\cdots(OC_6H_5)] \longleftrightarrow [(C_6H_6)\cdots(H^+\text{-}OC_6H_5)]$. *Cis*- and *trans*-type orientation of the two aromatic rings must be responsible for the presence of the two peaks in the IR spectra. A theoretical calculation with various basis sets is now going on for checking the validity of the assignment.

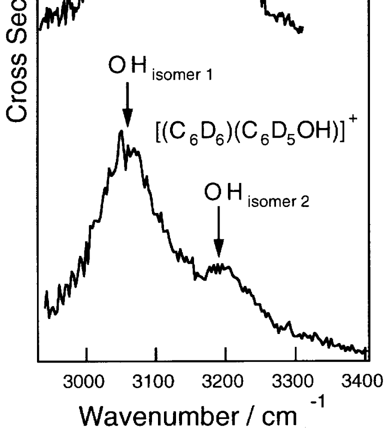

Figure 1. Photodissociation spectra of $[(C_6H_6)(C_6H_5OH)]^+$ (top) and $[(C_6D_6)(C_6D_5OH)]^+$ (bottom) in the IR region.